

## Dynamics of dislocation-mediated melting in a two-dimensional lattice in the presence of an oscillatory applied strain

A. J. Dahm, M. A. Stan, and R. G. Petschek

Physics Department, Case Western Reserve University, Cleveland, Ohio 44106

(Received 20 April 1989)

The temperature and frequency dependence of the power dissipated in a two-dimensional crystal subjected to an applied strain is shown to exhibit a distinct signature for dislocation-dissociation melting. The power absorption is analogous to the case of thin helium films subjected to an applied velocity field. Power loss by dislocation motion in the compressional mode is severely limited by the presence of nonequilibrium densities of interstitial and vacancy defects that are created or annihilated by dislocation climb. Tables of analogs between dislocations, vortices, and charges in two-dimensional systems are presented. The relation of the results to published experiments is discussed.

### I. INTRODUCTION

Halperin and Nelson<sup>1,2</sup> and Young<sup>3</sup> have developed an interesting and aesthetic theory of two-dimensional melting based on the ideas of Kosterlitz and Thouless.<sup>4</sup> This KTHNY theory predicts a continuous melting transition mediated by the breakup of dislocation pairs which exist as equilibrium defects in the crystal phase. This transition is from a crystalline phase to a hexatic liquid-crystal phase which contains free dislocations. The theory is particularly appealing because it makes a number of predictions which can be tested experimentally. Despite this fact, only a few experiments provide evidence that the breakup of dislocation pairs is responsible for the melting of any two-dimensional lattice, and here the evidence is not conclusive. Therefore, it is desirable to examine new experimental approaches to the study of melting of two-dimensional crystals. It is shown here that the absorption of power by the glide motion of dislocations, when a lattice is subjected to an applied strain, gives a distinct signature for KTHNY melting.

X-ray-scattering experiments on rare-gas atoms physisorbed on graphite suggest a continuous melting transition for coverages above one monolayer for argon,<sup>5</sup> krypton,<sup>6</sup> and for coverages above 0.9 monolayer for xenon.<sup>7-9</sup> Based on a molecular-dynamics simulation Koch and Abraham<sup>10</sup> conclude that one of these systems, an experiment on 1.1 monolayers of xenon,<sup>7,8</sup> undergoes a first-order transition, but mimics continuous behavior as a result of the interchange of atoms with the vapor. Also, one of the KTHNY parameters deduced from this experiment is anomalously small.<sup>11,12</sup> X-ray-scattering studies show evidence for a continuous transition to a hexatic liquid-crystal phase in monolayer xenon physisorbed on a sixfold-symmetric graphite surface<sup>13</sup> and on a weakly interacting silver (111) surface.<sup>14</sup> In the latter experiment the low-temperature phase was thought to be a hexatic glass resulting from pinning to steps or grain boundaries in the substrate. Some of these experimental results are contradicted by recent specific-heat measurements. Jin *et al.*<sup>15</sup> find a first-order specific-heat peak for coverages

both above and below 1 monolayer for xenon on graphite.

Continuous melting of submonolayer argon on graphite has been inferred from both x-ray-diffraction<sup>16</sup> and specific-heat<sup>17</sup> data. However, more precise specific-heat<sup>18</sup> measurements using a graphite foam substrate, which has a greater surface homogeneity, show a distinct first-order specific-heat peak. Continuous melting of ethylene on graphite has been attributed to a mechanism other than KTHNY melting.<sup>19</sup> The sum of the experimental evidence on adsorbed atoms is weighted against an interpretation in terms of KTHNY melting.

Murray and Van Winkle<sup>20</sup> made a visual observation of charged polystyrene spheres confined into two dimensions by two glass plates. The density of their sample varied continuously in space. They observed a two-step melting process with an intermediate phase which had the signature of a hexatic phase. The actual topological defects were more complex than those predicted by the KTHNY theory.

Strong evidence for a dislocation-mediated transition is provided by Deville *et al.*,<sup>21</sup> who measured the shear modulus  $\mu$  of a two-dimensional electron lattice as a function of frequency. The KTHNY theory predicts a rapid reduction of the shear modulus just below the transition temperature  $T_c$  and an abrupt discontinuity in the dc shear modulus at  $T_c$ . Deville *et al.* observed a reduction in  $\mu$  consistent with theoretical predictions as well as the expected increase in damping of the transverse mode as  $T_c$  is approached from below. Their signal amplitude decreased continuously, and their highest temperature detectable signal yielded a value of  $\mu$  in reasonable agreement with the theoretical value of  $\mu_{dc}(T_c)$ .

One difficulty with a measurement of the dc shear modulus is that a first-order melting mechanism such as grain boundary melting which is predicted to occur at a temperature  $T_g$  just below the dislocation-mediated transition temperature,<sup>22</sup> would yield the same temperature dependence of  $\mu_{dc}(T)$  up to  $T_g$ , where  $\mu_{dc}$  would abruptly vanish. This mimics the behavior predicted by the KTHNY theory. On the other hand, in the case of dislocation-mediated melting, the ac shear modulus is

predicted to decrease continuously to zero at a temperature  $T'_c > T_c$ . The measurements of Deville *et al.* were carried out at a finite frequency:  $\omega \sim 10^{-2} \omega_m$ , where  $\omega_m$  is the zone-boundary shear wave frequency. These authors report one data point below the stability line  $\mu_{dc}(T_c)$  versus  $T_c$ . This point might be interpreted as a finite frequency value above  $T_c$ .

Glattli *et al.*<sup>23</sup> measured the specific heat of the electron lattice in a very clever experiment. The specific heat varied continuously through the melting region as predicted by the KTHNY theory. They set an upper limit on the entropy discontinuity upon melting.

One other experimental result on the electron lattice, by some of the present authors and colleagues, has been interpreted as evidence in support of the KTHNY theory.<sup>24</sup> Guo *et al.* applied an alternating strain to the lattice, which was supported by a liquid-helium surface, and measured the power absorbed at various frequencies as a function of temperature. A sharp power absorption peak was measured in the vicinity of the melting transition. This anomalous power absorption was explained by the driven viscous motion of dislocations. The theory presented here was developed to analyze these results. A thermodynamic force, which limits dislocation climb and reduces the power absorbed by dislocation motion by orders of magnitude, was neglected in the previous analysis of Guo *et al.* We find that the maximum power absorbed by dislocation motion cannot account for the magnitude of the experimental anomalous absorption peak. Indirect effects of dislocations and dislocation pairs, such as ripplon scattering from dislocations, might explain these results.

The theory presented here is complementary to the theory of Zippelius *et al.*<sup>25</sup> on the response of a two-dimensional crystal to an applied stress. The details of the dynamics differ, and, in particular, the temperature dependence of the power absorbed by the dislocations above  $T_c$  differs dramatically. The response of dislocations to an applied strain is analogous to the response of vortices in a thin helium film to an applied superfluid velocity field.<sup>26</sup> This work relies heavily on the work of Ambegeokar, Halperin, Nelson, and Siggia (AHNS) on helium films<sup>26</sup> and of Zippelius, Halperin, and Nelson (ZHN) on the dynamics of melting.<sup>25</sup>

## II. THEORY

### A. Background

We wish to obtain an expression for the dissipation of energy arising from the motion of dislocations which are subject to an oscillating force. Such an expression has been derived by AHNS for the power absorbed by vortices in a thin helium film when driven by an oscillating force imposed via the coupling to the substrate. There are direct analogies between this system and dislocations in a lattice, and we adapt the theory of AHNS to determine the temperature and frequency dependence of the power absorbed by the driven motion of dislocations.

The AHNS and ZHN theories will be used extensively without making explicit references at each point.

According to the KTHNY theory of melting by the dissociation of dislocation pairs,<sup>27,28</sup> dislocation pairs exist as thermal equilibrium defects in two-dimensional crystals. These pairs polarize in the presence of an applied stress and reduce the strain field in the lattice, thereby causing a decrease in the elastic constants. The polarization of small pairs which are in close proximity to a large pair reduces the interaction energy of the larger pair. This screening is described by a dielectric constant  $\epsilon(r, T)$  which depends on the separation  $r$  of the two dislocations making up a pair. As the temperature approaches  $T_{KT}$  and the density of pairs increases,  $\epsilon(r, T)$  increases rapidly for large values of  $r$ . At the transition temperature  $T_{KT}$  some pairs dissociate ( $r \rightarrow \infty$ ) to form free dislocations. These free dislocations move in response to a stress and destroy the dc shear restoring force. Above  $T_{KT}$  the orientational order persists in a new phase designated as the hexatic liquid-crystal phase. The density of free dislocations  $n_f$  in this phase is<sup>2,26</sup>  $n_f^{-1} \approx 2\pi\xi_+^2$ , where the coherence length  $\xi_+$  varies with temperature as<sup>1-3</sup>

$$\xi_+ = \xi_0 \exp(b_0 t^{-\bar{\nu}}). \quad (1)$$

Here  $\xi_0$  and  $b_0$  are constants,  $b_0$  is related to the ratio<sup>12</sup>  $E_c/k_B T_{KT}$ , where  $E_c$  is the core energy of a dislocation,  $t$  is the reduced temperature, and the critical index  $\bar{\nu} = 0.37$ .

The energies of a free dislocation  $U_f$  and a dislocation pair  $U_p$  are given, respectively, by<sup>29</sup>

$$U_f = (Kb^2/8\pi) \ln(R/a) + E_c, \quad (2)$$

$$U_p = (Kb^2/4\pi) [\ln(r/a) - \cos^2\theta] + 2E_c. \quad (3)$$

Here  $\mathbf{b}$  is the Burgers vector  $\mathbf{b} = a\hat{\mathbf{b}}$ ,  $a$  is the lattice spacing,  $R$  is the radius of the system,  $\theta$  is the angle between the Burgers vector of one of the dislocations and the line joining the two dislocations, and the coupling constant  $K$  is given by

$$K(T) = 4\mu(\lambda + \mu)/(\lambda + 2\mu). \quad (4)$$

The Lamé constants  $\lambda$  and  $\mu$  are both renormalized by the presence of dislocations, and thus  $K$  is temperature dependent. The entropy of a free dislocation is given by  $S_f = k_B \ln(R/a)^2$ , and free dislocations enter the system when the free energy  $U_f - TS_f$  vanishes. This yields the following expression for the transition temperature:

$$T_{KT} = K(T)a^2/16\pi k_B. \quad (5)$$

### B. Power dissipation with the neglect of nonequilibrium net defect concentrations

We give here a microscopic derivation of the power dissipated by the motion of dislocations and obtain a standard macroscopic formula for power dissipated in a lattice. The total power absorbed by the dislocations is

the real part of the product of the force acting on a dislocation and its velocity summed over all dislocations. The force on a dislocation, given in terms of the stress components in cartesian coordinates  $\sigma_{ij}$ , is<sup>30</sup>

$$f_i = \epsilon_{ij} \sigma_{ij} b_i, \quad (6)$$

where  $\epsilon_{jl}$  is the antisymmetric tensor

$$\epsilon_{jl} = \begin{bmatrix} 0 & 1 \\ -1 & 0 \end{bmatrix}.$$

Summations are taken over repeated Latin indices.

The power dissipated per unit area in a crystal of area  $A$  is

$$p = \text{Re} \left\langle A^{-1} \sum_v \mathbf{f}^v \cdot \mathbf{v}^v \right\rangle_t, \quad (7)$$

where  $\mathbf{v}^v$  is the velocity of a dislocation located at coordinate  $\mathbf{R}^v$  and the brackets with a subscript  $t$  indicate a time average. We combine Eqs. (6) and (7) and use the relation  $\sigma_{ij} = \sigma_{ji}$  to obtain

$$p = \text{Re} \left\langle \sum_v \frac{b_i^v \sigma_{ij} \epsilon_{ij} v_i^v + b_j^v \sigma_{ij} \epsilon_{ji} v_j^v}{2A} \right\rangle_t. \quad (8)$$

The strain tensor  $u_{ij}$  is related to the displacement field  $\mathbf{u}(\mathbf{r})$  as

$$u_{ij}(\mathbf{r}) = \frac{1}{2} \left[ \frac{\partial u_i(\mathbf{r})}{\partial r_j} + \frac{\partial u_j(\mathbf{r})}{\partial r_i} \right]. \quad (9)$$

The contribution of dislocations to the integral of the strain component over the area of the lattice is given by

$$\int u_{ij} d^2 \mathbf{r} = \sum_v \frac{1}{2} (b_i^v \epsilon_{jl} R_l^v + b_j^v \epsilon_{il} R_l^v). \quad (10)$$

Since dislocations in the lattice can be combined in pairs, Eq. (10) is independent of the choice of origin. The time derivative of the average strain component  $\langle u_{ij} \rangle$  is therefore

$$\frac{d \langle u_{ij} \rangle}{dt} = A^{-1} \sum_v \frac{1}{2} (b_i^v \epsilon_{jl} v_l^v + b_j^v \epsilon_{il} v_l^v). \quad (11)$$

We multiply Eq. (11) by  $\sigma_{ij}$  and use the relation  $\epsilon_{jl} = -\epsilon_{lj}$ . A comparison of the result with Eq. (8) yields

$$p = -\text{Re} \left\langle \sigma_{ij} \frac{d \langle u_{ij} \rangle}{dt} \right\rangle_t. \quad (12)$$

In thermal equilibrium the stress tensor is related to the strain tensor by the elastic constants  $C_{ijkl}$ ,

$$(\sigma_{ij})_{\text{eq}} = C_{ijkl} u_{kl}. \quad (13)$$

The elastic stiffness constants are given by

$$C_{ijkl} = \mu(\delta_{ik} \delta_{jl} + \delta_{il} \delta_{jk}) + \lambda \delta_{ij} \delta_{kl}. \quad (14)$$

However, dislocations climb by creating or annihilating vacancy or interstitial defects. This results in a local deviation  $\delta c_\Delta$  from the equilibrium net defect concentration,  $c_\Delta$ . Here  $c_\Delta = c_i - c_v$ , and  $c_i$  and  $c_v$  are, respective-

ly, the interstitial and vacancy concentrations. ZHN include terms in  $\delta c_\Delta$  in the free-energy density of the crystal. For  $\delta c_\Delta / c_\Delta \ll 1$  these terms are

$$f_\Delta = \gamma u_{ii} \delta c_\Delta + (\delta c_\Delta)^2 / 2\chi, \quad (15)$$

where  $\gamma$  is a phenomenological coefficient. Upon dislocation climb, the increase in  $c_i$  and the decrease in  $c_v$  are in proportion to their equilibrium concentrations. With the relation  $\delta c_v / c_v = -\delta c_i / c_i$ , one finds for an ideal gas of defects,  $\chi^{-1} = n_0 k_B T / c_\Delta$ . Here  $n_0$  is the density of lattice sites and  $c_\Delta = c_i^0 + c_v^0$ , where the superscript 0 refers to the equilibrium concentrations.

The coupling between fluctuations in the net defect concentration and the strain field,  $\gamma u_{ii} \delta c_\Delta$ , results in an addition term in the expression for the reversible part of the stress tensor. The stress tensor is given by<sup>25</sup>

$$\sigma_{ij} = C_{ijkl} u_{kl} + \gamma \delta c_\Delta \delta_{ij}. \quad (16)$$

For the present, we shall neglect the second term in Eq. (16) and use Eq. (13) for the stress components. The effect of a finite value of  $\delta c_\Delta$  is to limit the climb motion of dislocations. This effect will be discussed later.

For an oscillating applied strain  $u_{ij} = u_{ij}^0 e^{-i\omega t}$ , the power dissipated per unit area is

$$p_0 = \frac{1}{2} \omega u_{ij}^0 \text{Im}(-C_{ijkl}) u_{kl}^0, \quad (17)$$

where the subscript 0 indicates that fluctuations in the defect deviation has been ignored. This is the standard expression for the power dissipation in a crystal. The temperature dependence of the elastic constants resulting from the presence of dislocation pairs is given by the KTHNY theory.

The rather formal equations (6) and (11) are easier to understand when the Cartesian components are written explicitly and applied to a particular dislocation. Consider a dislocation consisting of an extra half row of atoms, parallel to the  $y$  axis, in the upper half plane [see Fig. 1(a)]. By standard notation, this dislocation is assigned a Burgers vector  $\mathbf{b} = b\{1, 0\}$ . The force on this dislocation is

$$\mathbf{f}_{10} = \hat{\mathbf{x}} \sigma_{xy} b_x - \hat{\mathbf{y}} \sigma_{xx} b_x. \quad (18)$$

A positive shear stress moves the extra half row of atoms in the upper half plane in the direction of positive  $x$ , and a compression of the lattice along the  $x$  axis ( $\sigma_{xx} < 0$ ) attempts to exclude the extra half row by forcing it to move in the positive  $y$  direction.

The components  $d \langle u_{ij} \rangle / dt$  are

$$\frac{d \langle u_{xx} \rangle}{dt} = A^{-1} \sum_v b_x^v v_x^v, \quad (19a)$$

$$\frac{d \langle u_{yy} \rangle}{dt} = -A^{-1} \sum_v b_y^v v_y^v, \quad (19b)$$

$$\frac{d \langle u_{xy} \rangle}{dt} = -A^{-1} \sum_v \frac{1}{2} (b_x^v v_x^v - b_y^v v_y^v). \quad (19c)$$

Examples of lattices of length  $L$  and width  $W$  in strained

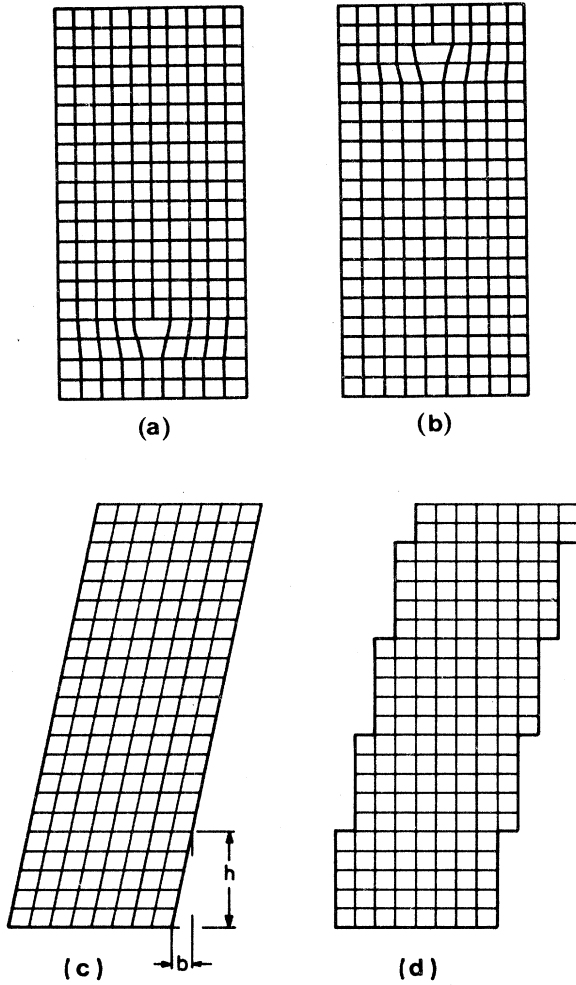


FIG. 1. Illustrations of crystals under a uniform strain: (a) compressional strain and (c) shear strain, and the respective crystals (b) and (d) after the strain has been relaxed by the motion of dislocations. Lattice sites are at the intersection of the lines.

states and in relaxed states following the motion of dislocations are shown in Fig. 1 to illustrate these equations. In Fig. 1(a) the lattice is compressed by an atomic spacing, and the resultant strain is  $u_{xx} = -b/W$ . The retraction of a dislocation with Burgers vector  $\mathbf{b} = \hat{x}b$  through a distance  $y$  alters the average strain by  $-u_{xx}y/L = b_x y/LW$ . This leads to a time rate of strain given by Eq. (19a), and Eq. (19b) follows from a cyclic permutation.

The relaxation of the shear strain can be understood with the aid of Figs. 1(c) and 1(d). The strain  $u_{xy} = b/2h$  changes by  $-b/2h$  when  $L/h$  dislocations with Burgers vector  $\mathbf{b} = \hat{x}b$  move a distance  $W$ . Thus  $u_{xy}$  changes by  $-b_x dx/2LW$  when one dislocation moves a distance  $dx$ . Likewise a dislocation with Burgers vector  $\mathbf{b} = \hat{y}b$  contributes an amount  $b_y dy/2LW$  when it moves a distance  $dy$ . The combination of these terms summed over all dislocations leads to Eq. (19c).

### C. Analogies with a two-dimensional plasma and with a thin helium film

It is pedagogically useful to draw analogies between dislocations in a two-dimensional crystal, vortices in a two-dimensional helium film, and charges in a two-dimensional plasma. To this end we reformulate the equation for the power absorption in the form of the electric analog.

The motion of dislocations in response to an applied stress polarizes the dislocations, i.e., dislocations with oppositely directed Burgers vectors move in opposite directions. We define a polarization tensor as<sup>31</sup>

$$P_{ij} = A^{-1} \sum_v \frac{1}{2} (b_i^\nu \epsilon_{lj} R_l^\nu + b_j^\nu \epsilon_{li} R_l^\nu). \quad (20)$$

The time derivative of the average stress due to the motion of dislocations is related to the time derivative of the strain by the bare elastic constants  $(C_{ijkl})_0$  which include all screening effects other than the motion of dislocations. The bare elastic constants enter here since the total motion of all charges including motion in response to the stress field of other charges is included in Eq. (11).

The time derivative of the average stress written in terms of the polarization is

$$\frac{d\langle \sigma_{ij} \rangle}{dt} = -(C_{ijkl})_0 \frac{dP_{kl}}{dt}. \quad (21)$$

An expression for the average stress is obtained by integrating Eq. (21) with respect to time,

$$\langle \sigma_{ij} \rangle = (C_{ijkl})_0 (u_{kl} - P_{kl}), \quad (22)$$

where  $\sigma_{ij}^{\text{ext}} = (C_{ijkl})_0 u_{kl}$  is the externally applied stress. The polarization tensor can be written in terms of the external field as

$$P_{kl} = \left[ 1 - \frac{C_{ijkl}}{(C_{ijkl})_0} \right] u_{kl}. \quad (23)$$

We proceed by making analogies with the equations describing a two-dimensional plasma. The average electric field  $\langle \mathbf{E} \rangle$  is related to the displacement field  $\mathbf{D}$ , which is applied by charging the capacitor plates by the relation

$$\langle \mathbf{E} \rangle = \epsilon_0^{-1} (\mathbf{D} - \mathbf{P}), \quad (24)$$

where  $\epsilon_0$  is the dielectric constant of the medium in which the plasma is embedded and does not include the screening due to the charges. The polarization  $\mathbf{P}$  is defined as

$$\mathbf{P} = A^{-1} \sum_v q^\nu \mathbf{R}^\nu. \quad (25)$$

The charge  $q^\nu$  located at coordinate  $\mathbf{R}^\nu$  takes on values  $\pm |q|$ . The polarization is related to the external field by

$$\mathbf{P}(\omega) = \{1 - [\epsilon_0/\epsilon(\omega)]\} \mathbf{D}(\omega), \quad (26)$$

where  $\epsilon(\omega)$  is the dielectric constant. The power dissipated per unit area for the case of an applied oscillatory displacement field at frequency  $\omega$  is

TABLE I. Equations for the properties of three analogous two-dimensional systems. The symbols are defined in the text.

Property	2D Coulomb gas	2D helium film	2D lattice
Energy of an isolated charge	$\frac{q^2}{4\pi\epsilon} \ln \left[ \frac{R}{a} \right] + E_c$	$\frac{\rho_s}{4\pi} \kappa^2 \ln \left[ \frac{R}{a} \right] + E_c$	$\frac{Kb^2}{8\pi} \ln \left[ \frac{R}{a} \right] + E_c$
Energy of a dipole	$\frac{q^2}{2\pi\epsilon} \ln \left[ \frac{r}{a} \right] + 2E_c$	$\frac{\rho_s}{2\pi} \kappa^2 \ln \left[ \frac{r}{a} \right] + 2E_c$	$\frac{Kb^2}{4\pi} \left[ \ln \left[ \frac{r}{a} \right] - \cos^2\theta \right] + 2E_c$
Field of an isolated charge	$\mathbf{E} = \frac{q}{2\pi\epsilon r} \hat{\mathbf{r}}$	$-\hat{\mathbf{z}} \times \mathbf{g}_s = \rho_s \frac{\kappa}{2\pi r} \hat{\mathbf{r}}$	$\sigma_{rr} = \sigma_{\theta\theta} = -\frac{Kb}{4\pi r} \sin\phi,$ $\sigma_{r\theta} = \frac{Kb}{4\pi r} \cos\phi$
Force on a charge	$\mathbf{f} = q\mathbf{E}$	$\mathbf{f} = -\rho_s \kappa \hat{\mathbf{z}} \times (\mathbf{v}_s - \mathbf{v}_c)$	$\mathbf{f}_i = \epsilon_{ij} \sigma_{ij} b_i$
Polarization	$\mathbf{P} = \sum_v \frac{q \mathbf{R}^v}{A}$	$\mathbf{P} = \sum_v \frac{\kappa^v \mathbf{R}^v}{A}$	$P_{kl} = \sum_v \frac{b_k^v \epsilon_{ml} R_m^v + b_l^v \epsilon_{mk} R_m^v}{2A}$
Time derivative of average field	$\frac{d\langle \mathbf{E} \rangle}{dt} = -\frac{1}{\epsilon_0} \frac{d\mathbf{P}}{dt}$	$-\hat{\mathbf{z}} \times d\langle \mathbf{g}_s \rangle / dt = -\rho_{s0} d\mathbf{P} / dt$	$d\langle \sigma_{ij} \rangle / dt = -(C_{ijkl})_0 dP_{kl} / dt$

$$p = (\omega/2) \text{Im}[-\epsilon^{-1}(\omega)] D_{\max}^2. \quad (27)$$

We compare the pairs of Eqs. (22) and (24), (20) and (25), and (23) and (26). By analogy we define

$$\epsilon_{ijkl}^{-1}(\omega) = C_{ijkl}(\omega). \quad (28)$$

The equation analogous to Eq. (27) is Eq. (17).

The similarities and differences in the three systems, dislocations, vortices, and charges, can be observed from the equations for the analogous properties which are given in Table I. The electric properties are in MKS units, and in this respect the definitions differ from those given by AHNS. The symbols in Table I which have not been defined are as follows: The electric charge  $q$  has dimension of charge/(length)<sup>1/2</sup>.  $\mathbf{g}_s = \rho_s \mathbf{v}_s$  is the superfluid momentum density,  $\rho_s$  and  $\mathbf{v}_s$  are, respectively, the superfluid density and velocity,  $\rho_{s0}$  is the bare superfluid density in the absence of vortices,  $\mathbf{v}_c$  is the velocity of the vortex core, and  $\hat{\mathbf{z}}$  is a unit vector normal to the helium film. The symbols  $R, r, a, \mathbf{R}^v, A$ , and  $\mathbf{P}$  have the same interpretation in each case. The circulation  $\kappa$  is Planck's constant divided by the atomic mass of helium and the signs refer to positive and negative circulation. The parameter  $E_c$  represents the self-energy of charges and the core energy of vortices. The angle  $\phi$  is measured counterclockwise from the Burgers vector. In writing the equations in Table I, the defects are assumed to be located at the center of a sample of radius  $R$  which is grounded in the case of a plasma, and the normal fluid in the helium films is assumed to be rest.

In Table II the transcriptions between these three systems are listed. Here  $\vec{\sigma}$  and  $\vec{u}$  are, respectively, the stress and strain tensors of the lattice. For an applied strain field, the analog of the dielectric constant is the elastic compliance tensor  $\vec{S}$ .

One can observe from Table I that the analogs between the properties of a two-dimensional crystal and the Coulomb gas and helium films are not exact. The

differences between dislocations and vortices are the following: dislocations in a triangular lattice have six possible orientations of the Burgers vectors whereas vortices are perpendicular to the film and have only two possible orientations. Secondly, dislocation triplets with zero Burgers vector sum can exist in a triangular lattice. These are incorporated as pairs by combining two nearby dislocations and treating this combination as a single dislocation in a pair. Thirdly, there is an angular strain introduced into the lattice by a dislocation and the stress is a tensor while the velocity field of a vortex is a vector and its magnitude depends only on the radial coordinate. Finally, dislocations differ in that they can only diffuse along the glide line in the absence of vacancies and interstitials, and their diffusion is one-dimensional on short time scales.

The predominant effect of the additional degrees of freedom of the Burgers vectors, the existence of triplets, and the angular strain field which leads to the  $\cos^2\theta$  term in the expression for  $U_p$  is to alter the form of the Kosterlitz-Thouless renormalization equations. The effects of the one-dimensional diffusion on short-time scales is to slightly alter the relaxation time for an ensemble of dislocation pairs when driven from a thermal equilibrium distribution.

Despite the differences between these systems, identical expressions are obtained for the dispersion relation and

TABLE II. Transcriptions for the parameters associated with three analogous two-dimensional systems. The symbols are defined in the text.

Parameter	Plasma	Helium film	Lattice
Defect	$q$	$\kappa = h/m$	$\mathbf{b}$
Dielectric constant	$\epsilon$	$\rho_s^{-1}$	$S_{ijkl}$
Fields	$\mathbf{E}$ $\mathbf{D}$	$-\hat{\mathbf{z}} \times \mathbf{g}_s$ $-\hat{\mathbf{z}} \times \mathbf{v}_s$	$\vec{\sigma}$ $\vec{u}$

the damping of third sound in thin superfluid films<sup>26</sup> and for the dispersion relation and the damping of transverse sound in a two-dimensional crystal.<sup>25</sup> These expressions are given in terms of the real and imaginary parts of the dielectric constant, and the differences lie in the forms of the Kosterlitz-Thouless renormalization curves from which the dielectric constant is calculated.

#### D. Dynamical dielectric constant

The absorbed power may be written as

$$p_0 = \frac{1}{2} \omega u_{ij}^0 u_{kl}^0 \frac{\epsilon''_{ijkl}}{(\epsilon'_{ijkl})^2 + (\epsilon''_{ijkl})^2}, \quad (29)$$

where  $\epsilon'$  and  $\epsilon''$  are, respectively, the real and imaginary parts of the dielectric constant. The dielectric constant is the sum of contributions from bound pairs and free dislocations,  $\epsilon(r) = \epsilon_b(r) + \epsilon_f$ . Only dislocation pairs contribute to  $\epsilon'$  while both pairs and free dislocations contribute to the losses and thus to  $\epsilon''$ . We will first examine the pair contribution to determine the correct value of  $r$  at which to evaluate  $\epsilon_b(r)$ .

For a given stress, the force acts in opposite directions on the two partners of a pair. Thus the pairs are alternately stretched and compressed in an alternating stress field. The maximum absorption occurs from those pairs for which  $\omega\tau(r, \theta) = 1$ , where  $\tau(r, \theta)$  is the characteristic time for an ensemble of pairs of separation  $r$  to relax to an equilibrium configuration after a stress field is removed. The relaxation time  $\tau(r, \theta)$  can be obtained by writing a pair of Langevin equations for the diffusive motion of a pair:<sup>32</sup>

$$dr_\mu/dt = -(2D_\mu/k_B T)(\nabla U)_\mu + \eta_\mu(t). \quad (30)$$

Here the subscript  $\mu$  refers to components parallel and perpendicular to the Burgers vectors. This equation is obtained by subtracting the Langevin equations for two dislocations of opposite sign moving in their mutual stress fields and subject to an oscillating external driving force  $\delta f_{\text{ext}}$ . Here  $U = U_p - \delta f_{\text{ext}} \cdot \mathbf{r}$ , where  $U_p$  is given by Eq. (3), and the parameter  $\eta(t)$  is a fluctuating Gaussian noise source with separate and unequal components along the glide and climb directions. The components  $\eta_j(t)$  along these directions satisfy

$$\langle \eta_\mu(t) \eta_\nu(t') \rangle = 2D_\mu \delta_{\mu\nu} \delta(t - t'). \quad (31)$$

Since locations can climb only by creating or annihilating defects, the diffusion coefficients for climb motion  $D_\perp$  and glide motion  $D_\parallel$  differ in magnitude. A dislocation climbs a distance  $a$  whenever a vacancy or interstitial moves to or from the dislocation. If the attractive interaction between a defect and a dislocation is neglected, this occurs at a frequency  $\omega_c = c_i \omega_i + c_v \omega_v$ , where  $\omega_i$  and  $\omega_v$  are, respectively, the interstitial and vacancy hopping frequencies, and  $D_i$  and  $D_v$  are their respective diffusion rates. The glide diffusion of the dislocations has been neglected here. The climb diffusion constant is  $D_\perp \approx c_\delta D_\delta \equiv c_i D_i + c_v D_v$ . The parameter  $D_\delta$  is an effective defect diffusion constant.

A crude estimate for  $\tau(r)$  can be obtained by setting the

time for an ensemble of pairs of separation  $r$  to relax to equilibrium after a stress is removed equal to  $\sim r/|dr/dt|$ . For the case  $\theta=0$ ,  $\nabla U_p = Kb^2/4\pi r$ , and  $\tau(r)$  is of the order of  $4\pi r^2 k_B T / 2DK (T_{\text{KT}}/b)^2 = r^2/8D$ .

Ambegaokar and Teitel<sup>32</sup> determined the response function  $g(r, \omega)$  for vortex pairs of separation  $r$  and fit  $g(r, \omega)$  to a single relaxation time  $g(r, \omega) \approx (1 - i\omega\tau)^{-1}$ . Their best fit gave  $\tau(r) = r^2/14D$ . The case for dislocation pairs differs from that for vortices in that  $D_\perp \ll D_\parallel$ , and the diffusion is essentially one dimensional on small-time scales.

Following the calculation of Ambegaokar and Teitel, we found  $g(r, \theta, \omega)$  for the one-dimensional diffusion of dislocation pairs along the glide line for the special case  $\theta=0$ . Our derivation is presented in the Appendix. This analysis ignores the interpair coupling. The best fit to  $g$  for a single relaxation time for  $\theta=0$  is  $\tau_\parallel(\theta=0) = r^2/15D_\parallel$ . For a given value of  $r$ , larger values of  $\theta$  are energetically favored. An analysis of our differential equation for  $g(r, \theta, \omega)$  suggests that  $g(r, \theta)$  will decrease for larger values of  $\theta$ . We suggest that the value for vortices,  $\tau_\parallel(r) = r^2/14D_\parallel$ , is a reasonable average value for dislocations. The solution for climb motion is difficult because the pair can undergo glide motion ( $r$  and  $\theta$  vary) in a climb relaxation time.

AHNS argue that since the response passes from its low- to high-frequency behavior at  $\omega\tau=1$  and  $\epsilon(r)$  is a slowly varying function of  $\ln r$ , the power losses may be approximated by evaluating  $\epsilon_b(r)$  at  $r = (14D/\omega)^{1/2}$ . They show that the imaginary part of  $\epsilon_b(\omega)$  is given by

$$\text{Im} \epsilon_b(\omega) = \frac{\pi}{4} \left[ r \left[ \frac{d\epsilon_b}{dr} \right] \right]_{r=(14D/\omega)^{1/2}}. \quad (32)$$

The contribution of free dislocations to the dielectric constant is taken from the plasma analog and is given by

$$\epsilon_f = i\sigma/\omega, \quad (33)$$

$$\sigma_\mu = n_f b^2 D_\mu / k_B T. \quad (34)$$

#### E. Effect of nonequilibrium defect concentrations on dislocation climb

The net defect concentration deviation  $\delta c_\Delta$  which enters Eq. (16) has been ignored in the above derivations. This deviation is proportional to the climb displacement of dislocations and reduces the applied force in the climb direction. The insertion of Eq. (16) for  $\sigma_{ij}$  into Eq. (12) yields the following expression for the power dissipated by climb motion:

$$p = p_0 - \omega \text{Im} \langle \gamma \delta c_\Delta u_{ii} \rangle. \quad (35)$$

An expression for  $\delta c_\Delta$  can be derived under certain conditions. The creation or annihilation of interstitials and vacancies by the motion of dislocations results in a local and temporal deviation in  $c_\Delta$  from equilibrium. Defects diffuse into a sample of dimension  $L$  from the boundaries on a time scale of  $\tau_L = L^2/D_\delta$ . If the climb motion of dislocations is sufficiently slow, this process will maintain  $\langle \delta c_\Delta \rangle \approx 0$ .

A uniform, but nonequilibrium, concentration of defects can be maintained if the defects created by the climb motion of dislocations diffuse sufficiently fast. The time scale to attain a uniform  $\delta c_\Delta$  is  $\tau_u \sim a^2/c_d D_\delta$ , where  $c_d$  is the concentration of dislocations. Both pairs and free dislocations are included in  $c_d$ .

We assume  $\delta c_\Delta$  to be uniform and small,  $|\delta c_\Delta/c_\delta| \ll 1$ , and define the climb of a dislocation as positive when an extra row of atoms is partially withdrawn. Positive climb then results in an increase in  $\delta c_\Delta$ . The time derivative of  $\delta c_\Delta$  is given by

$$\frac{d\langle \delta c_\Delta \rangle}{dt} = \hat{n} \cdot \sum_v \mathbf{b}^v \times \mathbf{v}^v, \quad (36)$$

where  $\hat{n}$  is a unit vector normal to the plane of the crystal. The product  $\mathbf{b} \times \mathbf{v} = \hat{n} b v_c$ , where the climb velocity  $v_c = f_c D_\perp / k_B T$ , and  $f_c$  is the net force in the climb direction. Only long-wavelength applied strains are considered here so that dislocation density gradients can be ignored.

The presence of a finite value of  $\delta c_\Delta$  leads to an excess pressure  $\bar{p}$  in the lattice,<sup>25</sup>

$$\bar{p} = \partial f_\Delta / \partial c_\Delta = \chi^{-1} \delta c_\Delta + \gamma u_{ii}. \quad (37)$$

The product  $-b\bar{p}$  represents an additional climb force on a dislocation. The term  $-b\chi^{-1}\delta c_\Delta$  represents a thermodynamic force which was first derived by Bardeen and Herring<sup>33</sup> for the case of vacancies. An increase (decrease) in  $c_\Delta$  results in a higher (lower) probability that an interstitial will diffuse to a dislocation and cause it to move against the applied force.

We consider only a uniform distribution of free dislocations so that we may neglect interdislocation forces. The climb force on a dislocation with a Burgers vector oriented at an angle  $\phi$  with respect to the  $x$  axis is

$$f_c = -b(\sigma_{xx} \cos^2 \phi + \sigma_{yy} \sin^2 \phi + \sigma_{xy} \sin 2\phi + \bar{p}). \quad (38)$$

This force can be written with the substitution of Eqs. (16) and (37) into Eq. (38) as

$$f_c = -b\{(B + \gamma)u_{ii} + \mu[(u_{xx} - u_{yy})\cos 2\phi + 2u_{xy}\sin 2\phi] + (\gamma + \chi^{-1})\delta c_\Delta\}. \quad (39)$$

Here  $B = \lambda + \mu$  is the bulk modulus. The time derivative of  $\langle \delta c_\Delta \rangle$  is obtained from Eqs. (36) and (39). The sum over dislocations averages over all angles, and we obtain

$$\frac{d\langle \delta c_\Delta \rangle}{dt} = -\tau^{-1}[(B + \gamma)u_{ii}/(\gamma + \chi^{-1}) + \langle \delta c_\Delta \rangle], \quad (40)$$

where the defect deviation relaxation time is

$$\tau = n_0 k_B T \chi / a^2 c_d D_\perp (1 + \gamma \chi) = \tau_u / (1 + \gamma \chi). \quad (41)$$

For an oscillatory applied strain, we obtain<sup>34</sup>

$$\langle \delta c_\Delta \rangle = -[(B + \gamma)/(\gamma + \chi^{-1})(1 - i\omega\tau)]u_{ii}. \quad (42)$$

The climb force on a dislocation vanishes in a time  $\tau$  after a strain is applied except for the angular-dependent term proportional to  $\mu$  in Eq. (39). The case for disloca-

tion pairs is much more complicated because intrapair forces must be included in Eq. (39). Nevertheless, the same qualitative behavior occurs, i.e., dislocation climb results in a net defect concentration deviation which builds up until the applied climb force is cancelled. In general, we may write

$$\langle \delta c_\Delta \rangle = -C(\omega, T)u_{ii}, \quad (43)$$

where  $C$  is complex both because of the finite value of  $\omega\tau$  and because it depends on the elastic constants.

The condition that the distribution of defects be uniform requires  $\omega\tau_u \ll 1$ . Equation (42) is valid in the range  $\tau_L^{-1} \ll \omega \ll \tau_u^{-1}$ . For larger frequencies, the local value of  $|\delta c_\delta|$  is large in the vicinity of dislocations undergoing climb motion, and their motion is again restricted.

The limitation  $|\delta c_\delta/c_\delta| \ll 1$ , assumed above, holds for small values of the applied compressional strain. We express  $\chi^{-1}$  with the use of Eqs. (4) and (5) as  $\chi^{-1} \sim \mu B / 4\pi(\mu + B)c_\delta$ . The limitation on  $u_{ii}^0$  such that  $|\delta c_\delta/c_\delta| \ll 1$  is

$$u_{ii}^0 \ll \frac{\mu}{4\pi(B + \mu)} \frac{1 + \gamma\chi}{1 + \gamma B^{-1}}. \quad (44)$$

#### F. Power dissipation including nonequilibrium net defect concentrations

In order to examine the power loss, we combine Eqs. (14), (17), (35), and (43) to break up the absorbed power into two terms,  $p = p_c + p_g$ , with

$$p_c = \frac{1}{2}\omega\{[\text{Im}(-B) - \text{Im}(-\gamma C)](u_{ii}^0)^2 + \frac{1}{2}\text{Im}(-\mu)[(u_{xx}^0 - u_{yy}^0)^2 + 4(u_{xy}^0)^2]\}, \quad (45)$$

$$p_g = \frac{1}{2}\omega\{\frac{1}{2}\text{Im}(-\mu)[(u_{xx}^0 - u_{yy}^0)^2 + 4(u_{xy}^0)^2]\}. \quad (46)$$

The respective applied force components along the climb and glide directions,  $f_c^a$  and  $f_g$ , are

$$f_c^a = -b\{(B - \gamma C)u_{ii} + \mu[(u_{xx} - u_{yy})\cos 2\phi + 2u_{xy}\sin 2\phi]\}, \quad (47)$$

$$f_g = -b\mu[(u_{xx} - u_{yy})\sin 2\phi - 2u_{xy}\cos 2\phi]. \quad (48)$$

The applied and net forces along the glide line are equal. The dislocation velocity is proportional to the net force acting on it. For the linear viscous response of dislocations to a force, the absorbed power is proportional to the real part of the dot product of the applied and net forces summed over all dislocations and averaged over all angles. A comparison of Eqs. (45) and (46) and the expressions for the average product of the respective applied and net force components allows one to identify Eqs. (45) and (46), respectively, as the power absorbed by the climb and glide motion of dislocations.

### III. DISCUSSION

An interesting result is the temperature dependence of the absorbed power for various frequencies of the applied

strain. The temperature dependence of the bulk and shear moduli are given by the KTHNY theory and are obtained from separate renormalization curves. The frequency dependence is determined by the pair separation at which the dielectric constants are evaluated.

The Kosterlitz-Thouless renormalization curves are functions of two variables which are parameteric in the variable  $l = \ln(r/a)$ , where  $a$  is the lattice spacing. The separation of a pair has little meaning for separations greater than the interpair spacing. The dislocations are considered to be free for larger separations,  $r > r^* \approx \xi_+ \propto \exp(l^*)$ , where  $l^* \approx b_0 t^{-\bar{\nu}}$  is calculated from the linearized renormalization curves.<sup>12</sup> The constant  $\xi_0$  in Eq. (1) is not known exactly, and we define

$$n_f = (f/2\pi a^2) \exp(-2l^*), \quad (49)$$

where  $f$  is a number of order unity. There are two other parameters in the theory. These are  $D$  and the ratio  $E_c/T = -\ln y_0$ , where  $y_0$  is the starting point for the integration of the renormalization curves.

#### A. Power losses due to glide motion

In Fig. 2 we present the temperature dependence of the power losses due to the driven glide of dislocations at various drive frequencies for the electron lattice. The figure is a plot of normalized power

$$\text{Im}(-\kappa_\mu^{-1}) = \kappa_\mu'' / [(\kappa_\mu')^2 + (\kappa_\mu'')^2], \quad (50)$$

where  $\text{Im}(-\mu) \approx \mu_0(T) \text{Im}(-\kappa_\mu^{-1})$ , and  $\kappa_\mu = \mu_0(T)/\mu(T) = \kappa' + i\kappa''$  is the relative dielectric constant for shear. Here  $\mu_0(T) \approx \mu_0(T_c)$  is the unrenormalized shear

modulus, i.e., in the absence of dislocations. It is about 10% greater than the critical value at  $T_{KT}$ . The parameters used in the calculation were  $f=1$ ,  $E_c/T_{KT}=4.9$ ,<sup>35</sup> and  $D_\parallel = \frac{1}{2}\omega_m a^2$ , where  $\omega_m$  is the transverse mode frequency averaged over the Brillouin zone boundary. The areal electron density was  $5.4 \times 10^8 \text{ cm}^{-2}$ . The justification for using this value of  $D_\parallel$  is that the energy for glide motion should be much less than  $E_c \sim 5k_B T$ , and thus the hopping frequency for dislocations is of the order of the attempt frequency  $\omega_m$ . The linearized renormalization curves were used for this figure. The full renormalization curves give the same qualitative behavior. They result in broader peaks and a slight shift of the peaks to higher temperature.

The power loss curves have a simple interpretation. A given lattice stress polarizes the dislocation pairs during each cycle of the external field. Those pairs which relax in a time  $\tau = \omega^{-1}$  dominate the power absorption at small reduced temperatures. The free dislocation density is strongly temperature dependent, and free dislocations give the dominant contribution at temperatures above the maximum when the more exact full renormalization curves are used. The contribution of free dislocations is small in the curves shown in Fig. 2.

The narrow width in temperature of the power absorption can be understood by examining Eq. (50). The components  $\kappa'(T)$  and  $\kappa''(T)$  both vary rapidly with temperature near  $T_{KT}$ , but the imaginary part  $\kappa'' \propto r d\kappa'/dr$  is vanishingly small for  $T \ll T_{KT}$  and varies much more rapidly than  $\kappa'$ . The ratio  $\kappa''/\kappa'$  varies from a negligible value to a value much greater than unity in a narrow range ( $\sim 10^{-2}$ ) of reduced temperature. As a result the

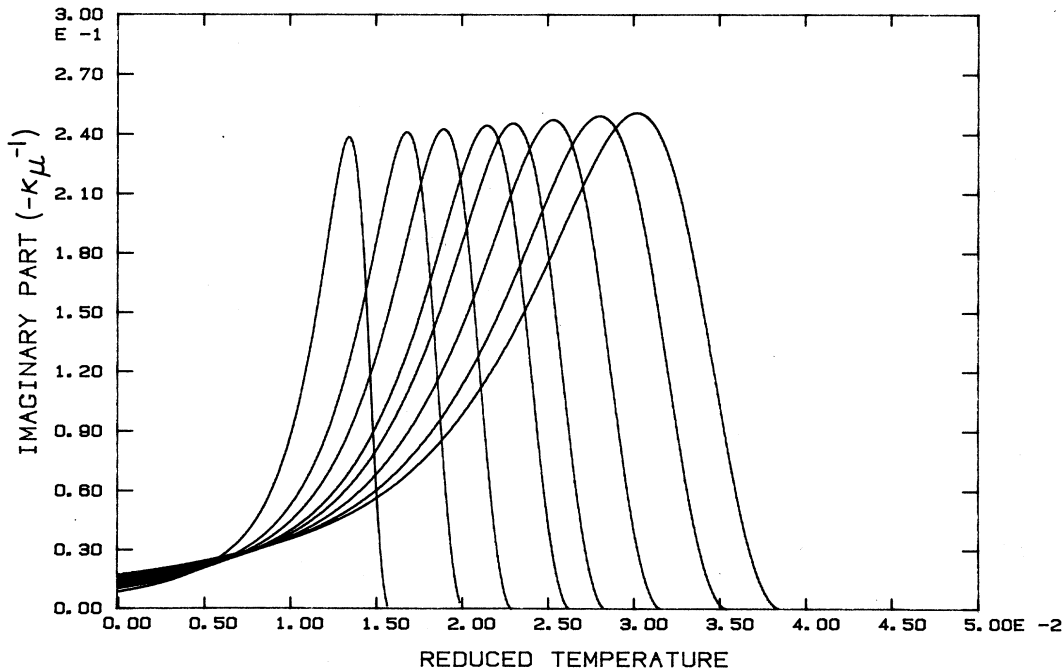


FIG. 2. Temperature dependence of the imaginary part of the relative dielectric constant for shear, Eq. (50), for a series of frequencies. The curves from left to right are for normalized applied frequencies  $\omega/\omega_m$  of 0.5, 2, 4, 8, 11.5, 19, 32, and  $45 \times 10^{-4}$ .



power loss is sharply peaked in temperature.

The shift of the peak to higher temperatures with increasing frequency is explained by the fact that the power absorption acts as a "spectrometer" which probes pairs with different separations at different drive frequencies,  $r \sim \omega^{-1/2}$ . Smaller pairs are probed at higher frequencies. Larger pairs are more strongly screened than smaller pairs at a fixed  $T$ . Thus a higher temperature (additional screening) is required to obtain the same value of the dielectric constant for smaller pairs. The contribution of free dislocations to  $\text{Im}(-\kappa_\mu^{-1})$  varies as  $\omega^{-1}n_f(T)$  on the low-temperature side of the peak and as  $\omega n_f^{-1}(T)$  in the high-temperature wing of the curve.

### B. Power losses due to climb motion

The contribution of pairs to the elastic constants must be evaluated at  $r = (\alpha_\perp D_\perp / \omega)^{1/2}$ , where  $\alpha_\perp$  is a numerical constant which we have not been able to evaluate. For  $\omega > \alpha_\perp D_\perp / a^2$ , the pair contribution to the loss from climb motion is greatly reduced. The pair contribution to the term proportional to  $\text{Im}(-\mu)$  in the expression for  $p_c$  is identical to the pair contribution to  $p_g$  with the frequency scaled by  $14D_\parallel / \alpha_\perp D_\perp$ . For the free dislocation contribution, the frequency is scaled by  $D_\parallel / D_\perp$ . The sum of  $p_g$  and this term in  $p_c$  result in broadened absorption peaks, or in the extreme case, a double peak.

The qualitative temperature dependence of  $\text{Im}(-B)$  is similar to  $\text{Im}(-\mu)$  but shifted to higher temperatures even neglecting the fact that  $D_\perp \neq D_\parallel$ . An exact evaluation of the term  $\text{Im}(-\gamma C)$  in Eq. (45) is difficult. The defect concentration in the electron lattice is small.<sup>35</sup> For this case the effect of the term  $\text{Im}(-\gamma C)$  is to nearly cancel the coefficient of  $(u_{ii}^0)^2$  in Eq. (45), since the creation of excess defects severely limits dislocation climb.

The large reduction in the power losses for an applied strain due to the creation of excess defects which occurs in the case of the electron lattice reflects the fact that only a small fraction of the total free energy of compression is associated with the rearrangement of "atoms." That is, the large value of bulk modulus is the result of long-range Coulomb interactions, and the bulk moduli for the fluid and crystal phases are nearly equal. Thus only a small fraction of the compressional energy can be extracted by the motion of dislocations.

### C. Relation to other work

The power absorption calculated here is analogous to the power absorption by vortices in a thin helium film when driven by a superfluid velocity flow.<sup>26</sup> The curves shown in Fig. 2 resemble the theoretical curves of AHNS which were evaluated by Bishop and Reppy.<sup>36</sup> The corresponding case of an applied stress was calculated by ZHN. For this case the power absorption is proportional to the imaginary part of the inverse elastic tensor coefficients. This leads to a monotonic increase in power absorption with temperature.

According to the work of AHNS, the finite frequency superfluid density decreases smoothly to zero at a temperature near the maximum of the absorption curve. The

finite frequency shear modulus, which is the analog of the superfluid density, should likewise vanish at a temperature near the absorption peak. Deville *et al.*<sup>21</sup> measured the temperature dependence of the shear modulus of the electron lattice at a frequency of  $\omega \sim 10^{-2}\omega_m$ . One observes from an extrapolation of the curves in Fig. 2 that their ac shear modulus should vanish at  $T \approx 1.04T_{KT}$ . Their single data point which lies below the stability line  $\mu_{dc}(T_{KT})$  versus  $T_{KT}$  might be interpreted as a finite frequency value above  $T_{KT}$ . Such an interpretation would presumably discriminate against a grain boundary mechanism and provide stronger evidence for dislocation-mediated melting of the electron crystal.

Together with colleagues, some of us reported<sup>24</sup> a measurement of the power absorbed by a two-dimensional electron lattice subjected to an applied uniaxial strain. A narrow frequency dependent absorption peak was observed in the vicinity of  $T_c$  with a reduced temperature width of  $\sim 0.05$ . The maximum power absorbed per unit area at an applied frequency of 1 MHz was  $4 \times 10^{-9}$  W/m<sup>2</sup> for an applied strain of  $u_{xx}^0 = 2 \times 10^{-5}$ ,  $u_{yy}^0 = u_{xy}^0 = 0$ . The shear and bulk moduli for this sample are calculated to be  $\mu_0 = 4 \times 10^{-10}$  J/m<sup>2</sup> and  $B = 10^5 \mu$ . According to Eqs. (46) and (50) and Fig. 2, the maximum power absorbed by the glide motion of dislocations is  $\sim 6 \times 10^{-14}$  W/m<sup>2</sup>. An equal amount of power is accounted for by the second term in the brackets of Eq. (45), and the first term is not substantially larger because of cancellation by the thermodynamic force. The power absorbed by dislocation motion fails to account for the peak power absorption by four orders of magnitude.

If it should prove possible to find a two-dimensional system in which the damping due to dislocation motion throughout the melting region is not overwhelmed by other loss mechanisms, the temperature- and frequency-dependent response to an applied strain will provide a strong test of dislocation-mediated melting. In particular, it is the limitation on losses by dislocation climb resulting from a net defect concentration deviation, which allows for a high- $Q$  (quality factor) response. Thus the response to a compressional strain can, in principle, be measured well above  $T_c$  without overdamping.

We have examined the imaginary part of  $\epsilon^{-1}$  to obtain the temperature and frequency dependence of the power absorption. The temperature dependence of the finite frequency shear modulus under conditions of applied strain can be obtained from the real part of  $\epsilon^{-1}$ . A measurement of the frequency dependence of the shear modulus in the region of melting would provide a further test of dislocation-mediated melting.

### ACKNOWLEDGMENTS

One of the authors (A.J.D.) acknowledges valuable discussions with K. Binder and H. Weichert and wishes to thank P. Leiderer and the University of Mainz for their hospitality and the Fulbright Commission for support during the writing of this manuscript. This work was supported by the National Science Foundation under Grant No. 82-13581.

### APPENDIX: RELAXATION OF DISLOCATION PAIRS

We are interested in calculating the linear response of a thermal ensemble of dislocation pairs to an oscillating applied force. We shall only consider glide motion. This derivation follows the analysis of the relaxation of vortex pairs in a helium film by Ambegaokar and Teitel<sup>32</sup> and differs from it in that the diffusion in the present case is one dimensional since dislocations are restricted to move along the glide line, i.e., parallel to the Burgers vectors. The interactions between pairs are neglected:

$$U_p = 2q^2 \int_a^r \frac{dr}{\epsilon(r)r} - \frac{2q^2}{\epsilon(r)} \cos^2 \theta - q \delta \mathbf{E} \cdot \mathbf{r} + 2E_c, \quad (\text{A1})$$

where  $2q^2/\epsilon(r) = Kb^2/4\pi$ ,  $\epsilon(r)$  is the static dielectric constant,  $\delta E$  represents a small macroscopic stress in the lattice, which varies as  $e^{-i\omega t}$ , and the separation of a pair  $r$  and the angle  $\theta$  are shown in Fig. 3.

We consider a pair whose glide lines are separated by a constant distance  $y = r \sin \theta$ . The Langevin equation for the pair is

$$\frac{dx}{dt} = 2DF_x/k_B T + \eta(t), \quad (\text{A2})$$

where  $D = D_{\parallel}$  and  $\eta$  is a Gaussian noise source obeying Eq. (31). The force along the glide line is given by  $F_x = -(\partial U/\partial x)|_y = \text{const}$ . This leads to

$$F_x = -\lambda 2q^2/\epsilon x - q \delta E_x = F_{x0} + \delta F_x, \quad (\text{A3})$$

where  $\lambda(x) = \cos^2 \theta \cos 2\theta = x^2(x^2 - y^2)/(x^2 + y^2)^2$ .

The density of pairs per unit area of separation is

$$\Gamma(r, \theta, t) = a^{-4} \exp[-U(r, \theta, t)/k_B T]. \quad (\text{A4})$$

We write  $U = U_0 - q \delta \mathbf{E}(t) \cdot \mathbf{r}$  and  $\Gamma = \Gamma_0 + \delta \Gamma$  from which we obtain

$$\Gamma = \Gamma_0 [1 + q \delta E_x x g(x, \omega)/k_B T], \quad (\text{A5})$$

where  $g(x, \omega) = 1$  corresponds to local equilibrium. Thus

$$\delta \Gamma = q \delta E_x x \Gamma_0 g(x, \omega)/k_B T \quad (\text{A6})$$

and we ignore the term  $\exp(q \delta E_y y/k_B T)$  since the dislocations cannot respond to the  $y$  component of the field on short-time scales and this term is oscillatory and approximately equal to unity.

The continuity equation for  $d\Gamma/dt$  is

$$\frac{d\Gamma}{dt} = -\nabla \cdot (\Gamma d\mathbf{r}/dt), \quad (\text{A7})$$

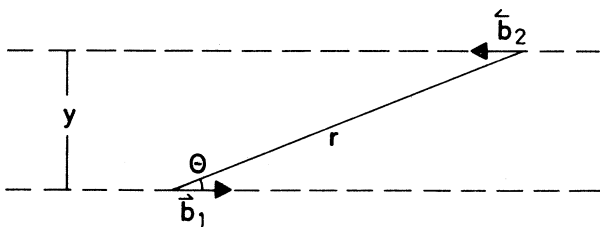


FIG. 3. Geometry of a dislocation pair defining  $r$ ,  $\theta$ , and  $y$ . The dashed lines represent glide lines.

which leads to the Fokker-Planck equation for  $\Gamma$ ,

$$\frac{d\Gamma}{dt} = \frac{2D}{k_B T} \frac{d}{dx} (\Gamma F_x) + 2D \frac{d^2 \Gamma}{dx^2}. \quad (\text{A8})$$

Equation (A8) is solved for small deviations from equilibrium as

$$-i\omega \delta \Gamma = -\frac{2D}{k_B T} \frac{\partial}{\partial x} (\Gamma_0 \delta F_x + F_{x0} \delta \Gamma) + 2D \frac{\partial^2 \delta \Gamma}{\partial x^2}. \quad (\text{A9})$$

By substitution of previously defined quantities into Eq. (A9),  $g$  is found to obey the differential equation

$$x^2 g'' + x(2-s)g' - (-i\omega x^2/2D + s)g + s = 0, \quad (\text{A10})$$

where  $s = \lambda(x)2q^2/\epsilon k_B T$ .

As a first approximation, we set  $2q\epsilon k_B T = 2q^2/\epsilon_c k_B T_c = 4$  and define  $z^2 = -i\omega x^2/2D$ . Then Eq. (A9) takes the form

$$z^2 g''(z) - [4\lambda(z) - 2]zg'(z) - [4\lambda(z) + z^2]g(z) + 4\lambda(z) = 0. \quad (\text{A11})$$

This equation may be compared with Eq. (9) of Ambegaokar and Teitel.<sup>32</sup> The difference between the numbers 2 and 3 appearing in the coefficients of  $xg'$  in Eq. (A10) and Eq. (7) of Ref. 32 arises from the difference in the one- and two-dimensional Laplacians used, respectively, in Eq. (A9) and Eq. (5) of Ref. 32.

It is very difficult to solve Eq. (A11) in general, and we examine only the limiting case:  $p \simeq 0$ ,  $\lambda = 1$ ,  $y = 0$ , and  $x = r$ . Equation (A11) has a resonance at  $\lambda = 1$ . Instead of solving this case directly we solve the differential equation for fixed  $\lambda$  and define

$$g(\lambda = 1) = \lim_{\delta \rightarrow 0} g(\lambda = 1 - \delta). \quad (\text{A12})$$

The particular solution which is equal to unity at  $z = 0$  can be generated by a power series. The result can be written as

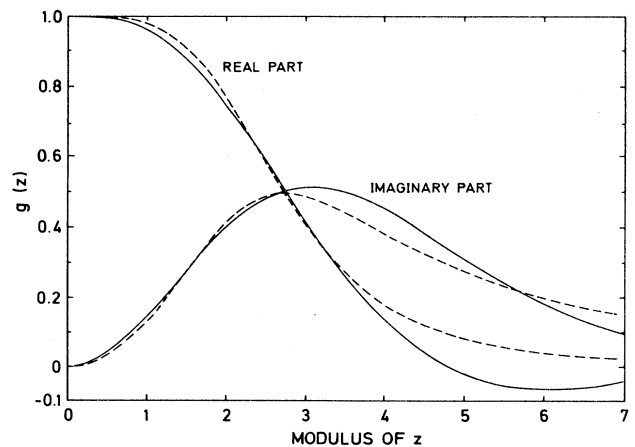


FIG. 4. Response function  $g(z)$  vs modulus of  $z$  for  $\theta = 0$ . The solid lines represent the exact solution  $g(z)$ . The dashed lines are given by an approximate solution  $g = (1 - i\omega r^2/15D)^{-1}$ .

$$g_p(z) = 1 + \Gamma(3/2)\Gamma(1-2\lambda) \times \sum_{n=1}^{\infty} \frac{(z/2)^{2n}}{\Gamma(n+3/2)\Gamma(n+1-2\lambda)}, \quad (\text{A13})$$

where  $\Gamma(k)$  is the gamma function. The homogeneous solution which is regular at the origin is

$$g_n(z) = z^p I_\nu(z), \quad (\text{A14})$$

where  $p = 2\lambda - \frac{1}{2}$  and  $I(z)$  is a modified Bessel function of order  $\nu = 2\lambda + \frac{1}{2}$ .

The general solution which is regular at the origin is

$$g(z) = g_p(z) + \kappa g_n(z). \quad (\text{A15})$$

The constant  $\kappa$  is determined by setting  $g(z) = 0$  as  $z \rightarrow \infty$ . The asymptotic behavior of the particular solution is

$$\lim_{z \rightarrow \infty} g_p(z) \simeq \Gamma(3/2)\Gamma(1-2\lambda)2^{-p}z^p I_{1-\nu}(z). \quad (\text{A16})$$

Since all orders of  $I_\nu$  have the same asymptotic behavior, the constant  $\kappa$  is

$$\kappa = -2^{-p}\Gamma(3/2)\Gamma(1-2\lambda). \quad (\text{A17})$$

In Fig. 4 we plot the real and imaginary parts of  $g$  ( $\lambda = 0.98$ ) as a function of  $(\omega x^2/2D)^{1/2}$ . Also shown is the best fit to a single relaxation time given by  $g = [1 - i\omega\tau(0)]$  with  $\tau(\theta=0) = r^2/15D$ .

- <sup>1</sup>D. R. Nelson, Phys. Rev. B **18**, 2318 (1978).
- <sup>2</sup>B. I. Halperin and D. R. Nelson, Phys. Rev. Lett. **41**, 121 (1978); **41**, 519(E) (1978); D. R. Nelson and B. I. Halperin, Phys. Rev. B **19**, 2457 (1979).
- <sup>3</sup>A. P. Young, Phys. Rev. B **19**, 1855 (1979).
- <sup>4</sup>J. M. Kosterlitz and D. J. Thouless, J. Phys. C **6**, 1181 (1973); J. M. Kosterlitz, *ibid.* **7**, 1046 (1974).
- <sup>5</sup>H. Taub, K. Carneiro, J. K. Kjems, and L. Passell, Phys. Rev. B **16**, 4551 (1977); J. P. McTague, J. Als-Nielsen, J. Bohr, and M. Nielsen, *ibid.* **25**, 7765 (1982).
- <sup>6</sup>E. D. Specht, M. Sutton, R. J. Birgeneau, D. E. Moncton, and P. M. Horn, Phys. Rev. B **30**, 1589 (1984).
- <sup>7</sup>P. A. Heiney, R. J. Birgeneau, G. S. Brown, P. M. Horn, D. E. Moncton, and P. W. Stephens, Phys. Rev. Lett. **48**, 104 (1982).
- <sup>8</sup>P. A. Heiney, P. W. Stephens, R. J. Birgeneau, P. M. Horn, and D. E. Moncton, Phys. Rev. B **28**, 6416 (1983).
- <sup>9</sup>P. Dimon, P. M. Horn, M. Sutton, R. J. Birgeneau, and D. E. Moncton, Phys. Rev. B **31**, 437 (1985).
- <sup>10</sup>S. W. Koch and F. F. Abraham, Phys. Rev. B **27**, 2964 (1983); F. F. Abraham, Phys. Rev. Lett. **50**, 978 (1983); Phys. Rev. B **29**, 2606 (1984).
- <sup>11</sup>The value of  $B$ ,  $0.08 \leq B \leq 0.22$ , defined in Eq. (13) of Ref. 8 is unexpectedly small. See Fig. 2 in Ref. 12. The parameter  $B$  of Ref. 8 is denoted by  $b$  in this figure.
- <sup>12</sup>A. J. Dahm, Phys. Rev. B **29**, 484 (1984).
- <sup>13</sup>T. F. Rosenbaum, S. E. Nagler, P. M. Horn, and R. Clarke, Phys. Rev. Lett. **50**, 1791 (1983); S. E. Nagler, P. M. Horn, T. F. Rosenbaum, R. J. Birgeneau, M. Sutton, S. G. J. Mochrie, D. E. Moncton, and R. Clarke, Phys. Rev. B **32**, 7373 (1985).
- <sup>14</sup>N. Greiser, G. A. Held, R. Frahm, R. L. Greene, P. M. Horn, and R. M. Suter, Phys. Rev. Lett. **59**, 1706 (1987).
- <sup>15</sup>A. J. Jin, M. R. Bjurstrom, and M. H. W. Chan, Phys. Rev. Lett. **62**, 1372 (1989).
- <sup>16</sup>C. Tiby and H. J. Lauter, Surf. Sci. **117**, 277 (1982).
- <sup>17</sup>T. T. Chung, Surf. Sci. **87**, 348 (1979).
- <sup>18</sup>A. D. Migone, Z. R. Li, and M. H. W. Chan, Phys. Rev. Lett. **53**, 810 (1984).
- <sup>19</sup>J. Z. Larese, L. Passell, A. D. Heidemann, D. Richter, and J. P. Wicksted, Phys. Rev. Lett. **61**, 432 (1988).
- <sup>20</sup>C. A. Murray and D. H. Van Winkle, Phys. Rev. Lett. **58**, 1200 (1987).
- <sup>21</sup>G. Deville, A. Valdes, E. Y. Andrei, and F. I. B. Williams, Phys. Rev. Lett. **53**, 588 (1984).
- <sup>22</sup>S. T. Chui, Phys. Rev. Lett. **48**, 933 (1982); Phys. Rev. B **28**, 178 (1983).
- <sup>23</sup>C. D. Glatli, E. Y. Andrei, and F. I. B. Williams, Phys. Rev. Lett. **60**, 420 (1988).
- <sup>24</sup>C. J. Guo, D. B. Mast, R. Mehrotra, Y. Z. Ruan, M. A. Stan, and A. J. Dahm, Phys. Rev. Lett. **51**, 1461 (1983); D. B. Mast, C. J. Guo, M. A. Stan, R. Mehrotra, Y. Z. Ruan, and A. J. Dahm, Surf. Sci. **142**, 100 (1984).
- <sup>25</sup>A. Zippelius, B. I. Halperin, and D. R. Nelson, Phys. Rev. B **22**, 2514 (1980).
- <sup>26</sup>V. Ambegoakar, B. I. Halperin, D. R. Nelson, and E. D. Sigia, Phys. Rev. Lett. **40**, 783 (1978); Phys. Rev. B **21**, 1806 (1980).
- <sup>27</sup>A lucid description of the Kosterlitz-Thouless theory and its application to both two-dimensional crystals and thin films including the dynamics of vortices is given by B. I. Halperin, in *Physics of Low-Dimensional Systems*, edited by Y. Nagaoka and S. Hikami (Kyoto University, Kyoto, 1979), p. 53.
- <sup>28</sup>A detailed description of defect-mediated phase transitions is given by D. R. Nelson, in *Phase Transitions and Critical Phenomena*, edited by C. Domb and J. L. Lebowitz (Academic, New York, 1983), Vol. 7, p. 1.
- <sup>29</sup>F. R. N. Nabarro, *Theory of Crystal Dislocations* (Clarendon, New York, 1967).
- <sup>30</sup>J. S. Peach and J. M. Koehler, Phys. Rev. **80**, 436 (1950).
- <sup>31</sup>R. Bruinsma, B. I. Halperin, and A. Zippelius, Phys. Rev. B **25**, 579 (1982).
- <sup>32</sup>V. Ambegoakar and S. Teitel, Phys. Rev. B **19**, 1667 (1979).
- <sup>33</sup>J. Bardeen and C. Herring, in *Imperfections in Nearly Perfect Crystals*, edited by W. Shockley, J. H. Hollomon, R. Maurer, and F. Seitz (Wiley, New York, 1952), p. 261.
- <sup>34</sup>Equation (42) may be compared to the  $k=0$  limit of Eqs. (5.25) and (5.26) of Ref. 25. The discrepancy of a factor of 2 results from a double counting which originates in Eq. (4.44) of Ref. 25.
- <sup>35</sup>D. S. Fisher, B. I. Halperin, and R. Morf, Phys. Rev. B **20**, 4692 (1979).
- <sup>36</sup>D. J. Bishop and J. Reppy, Phys. Rev. Lett. **40**, 1727 (1978); Phys. Rev. B **22**, 5171 (1980).